ELSEVIER

Fluid Phase Equilibria 183–184 (2001) 363–370

FLUID PHASE EQUILIBRIA

www.elsevier.com/locate/fluid

Characterizing the viscosity–temperature dependence of lubricants by molecular simulation

Clare McCabe [a,b,*], Shengting Cui [a,b], Peter T. Cummings [b,c]

[a] *Department of Chemical Engineering, University of Tennessee, Knoxville, TN 37996-2200, USA*
[b] *Chemical Technology Division, Oak Ridge National Laboratory, Oak Ridge, TN 37831-6181, USA*
[c] *Departments of Chemical Engineering, Chemistry and Computer Science, University of Tennessee, Knoxville, TN 37996-2200, USA*

Abstract

An understanding of the relationship between chemical structure and lubricant performance is highly desirable from both a fundamental and a practical perspective, such knowledge being vital to improve the performance of mineral oils and to guide the design of future synthetic lubricants. The rheological properties of alkanes of intermediate molecular size (C_{20}–C_{40}) are of particular interest as they form the main constituents of lubricant basestocks. In this work, we determine the viscosity number (VN) for a number of alkanes in the mass range of interest by molecular simulation. Quantitative agreement with experimental data for all systems studied is achieved, further illustrating the value of molecular simulation in predicting lubricant properties and its potential for providing guidance in the design of synthetic lubricants with desired properties.

Keywords: Molecular dynamics; Simulation; Alkanes; Viscosity number

1. Introduction

Lubricants and lubrication techniques are an indispensable feature of all machinery, ranging from applications which enable the manipulation of very small parts to the movement of very heavy masses. The diverse nature of operating conditions necessitates that the lubricant for a specific practice be very carefully chosen in order to match the working requirements, for example, in the automobile engine the lubricant must be operational over a very wide temperature, speed, and load.

The general move towards more severe operating conditions in a drive for greater economics and overall efficiency has led to an increase in the significance of lubricant viscosity, and more specifically lubricant behavior with changing temperatures. Although viscosity is only one of many factors taken into

* Corresponding author. Tel.: +1-865-974-0227; fax: +1-865-974-4910.
E-mail address: clare@utk.edu (C. McCabe).

0378-3812/01/$20.00
PII: S0378-3812(01)00448-4

account in the characterization of lubricant performance, it is essential that a lubricant has a sufficiently high viscosity at normal operating temperatures (for example, temperatures up to 100°C in the case of an automobile engine), whilst not being excessively high at the lowest temperatures (for example, a cold start in the case of an automobile). The ideal lubricant would be one whose viscosity was minimally affected by the range of operating temperatures encountered: though in reality viscosity changes substantially with temperature, depending on the chemical and physical properties of the lubricant.

In the past, numerous methods have been suggested for expressing the variation of viscosity with temperature [1]. Perhaps the most common is the viscosity index (VI) proposed by Dean and Davis [2] in 1929. Generally, the higher the VI of a substance the less it is affected by changes in temperature, and therefore, the better the potential lubricant, though we note that the VI should not be considered alone. For example, linear alkanes have a high VI but because of their high melting points, they have a high pour point, and are therefore, not useful as lubricants in most practical applications since they are solids at ambient conditions.

The VI system was first revised by Hardiman and Nissan [3], in order to overcome problems encountered with the original VI scheme at high VI and low viscosity. They proposed an empirical relation, which although applicable to a wider range of oils, was never adopted as the ASTM standard. The current ASTM standard method (D2270-93) for determining the VI is based on the method of Dean and Davis, and involves the comparison of the kinematic viscosity of the test substance with that of two reference oils at 40 and 100°C. The VI system in its present form is widely used to compare lubricants, however, it suffers a major drawback in that it is undefined for lubricants with a kinematic viscosity less than 2 cSt at 100°C.

The viscosity number (VN) was recently proposed as an alternative measure of lubricant performance. It is applicable over a wider range of temperatures and has been shown to correlate well with the VI [4]. As with the VI scale the larger the VN the smaller the change in viscosity with temperature, and hence the 'better' the test substance will perform as a lubricant. Given the kinematic viscosity at 40 and 100°C, in a similar manner to the calculation of the VI, the kinematic viscosity at these two temperatures is substituted into the Walther equation

$$\log\log(v + 0.7) = A + B\log T \tag{1}$$

where v is the kinematic viscosity and T the temperature. Once the coefficient B has been determined from Eq. (1) the VN can be easily obtained using the equation

$$\mathrm{VN} = \left(1 + \frac{3.55 + B}{3.55}\right) \times 100 \tag{2}$$

Over the last decade, there have been a number of simulation studies reported in the literature on the rheological properties of industrially important molecules [5], such as the alkanes, though early work was limited to short, mainly linear molecules (see, for example [6–10]). However, with the recent advances in computational power, and the development of more realistic models and suitable algorithms it is now possible to perform simulations of more complex systems. Recently, longer chains and branched molecules have been examined [7,11–16], leading to the opportunity to gain molecular level insight into questions of industrial relevance. For example, the VI of linear alkanes increases with chain length, but how does the introduction of branching impact the pour point and the VI [17,18]? Given the limited available experimental data, computer simulation studies are an attractive means to obtain valuable information on the complex relationship between molecular architecture and viscous behavior. Furthermore, the

conditions commonly met in practical applications, such as automobile engines and machinery (e.g. giga-pascal pressures and nanoscale gaps between surface asperities) are very difficult to achieve and study experimentally, but pose far fewer problems in a computer "experiment".

The first prediction of the VI by molecular simulation was performed by this group [15] using the united atom model of Smit and coworkers [19,20] with the extension to branched alkanes by Mondello and Grest [21]. Excellent agreement was obtained between simulation and experimental data for structural isomers of $C_{30}H_{62}$ [15,18]. Later, Kioupis and Maginn predicted the VN for three structural isomers of $C_{18}H_{38}$ by molecular simulation using the united atom transferable potentials for phase equilibria (UA-TraPPE) force field model [17]. Although experimental data was only available for the VN of linear octadecane good agreement was obtained between simulation and experiment.

In this work, we present the results of equilibrium (EMD) and nonequilibrium molecular dynamics (NEMD) simulations of 9-octylheptadecane, a star-like isomer of $C_{25}H_{52}$. Additionally, we determine the VN for 9-octylheptadecane, and for 9-octyldocosane and squalane using previous simulation results, obtaining excellent agreement with experimental data.

2. Simulation details

The model used to describe the alkane molecules is that of Siepmann and coworkers [19,20], which was later extended to branched alkanes by Mondello and Grest [21]. As in earlier work [10], we use the modification of Mundy and coworkers in which the fixed bond length is replaced by a stiff harmonic potential to generate a fully flexible model [9]. We will briefly describe the model and the simulation methods, though the reader is directed to the original papers for full details.

In this united atom description of the alkanes, the methyl, methylene and methyne groups are recognized and individually treated as single spherical interaction sites with the interaction center located at the center of each carbon atom. A Lennard–Jones (LJ) potential describes the intermolecular interactions, and the intramolecular interactions between sites separated by three or more bonds. A cut off distance of 9.85 Å ($2.5\sigma_{CH_2}$) was used. The potential model size and energy parameters can be found in Table 1. Simple Lorentz–Berthelot combining rules were used to determine the cross or unlike interactions. Bond stretching is described by a harmonic potential with an equilibrium bond distance of $r_{eq} = 1.54$ Å and force constant $k_a/k_B = 4{,}529{,}000\,\mathrm{K\,rad^{-2}}$ (where k_B is Boltzmann's constant). The bond angle bending term is also described by a harmonic potential with an equilibrium angle of $\theta_{eq} = 114^\circ$ and force constant $k_b/k_B = 62{,}400\,\mathrm{K\,rad^{-2}}$. In the extension to branched alkanes by Mondello and Grest [21], an *ad hoc* harmonic potential similar to the bending term was introduced to prevent the unphysical umbrella inversion of the tertiary carbon atoms ($\theta = 27.25^\circ$ and $k_c/k_B = 40{,}258\,\mathrm{K\,rad^{-2}}$). Finally, torsional

Table 1
Lennard–Jones potential model parameters

United atom	σ (Å)	ε/k_B (K)
CH_3	3.93	114
CH_2	3.93	47
CH	3.81	40

Table 2
Torsional potential parameters

	a_0/k_B (K)	a_1/k_B (K)	a_2/k_B (K)	a_3/k_B (K)
X–CH_2–CH_2–Y	1010	2019	136.4	−3165
X–CH–CH_2–Y	409.6	901.8	195.8	−1848

motion characterizing the preferred orientational and rotational barriers around all nonterminal bonds is described through the potential of Jorgensen (Table 2).

The alkanes were simulated under planar Couette flow using the SLLOD equations of motion with a Nosé thermostat. The multiple time step technique from the work of Tuckerman et al. [22] and Cui et al. [23] was used to integrate the equations of motion, all the intramolecular interactions were treated as fast motions and the intermolecular interactions as the slow motion. For the fast mode motion a time step of 0.235 fs was used, and for the slow mode motion the time step was 2.35 fs. To generate the starting configurations, each atom was given a small LJ diameter and the molecules placed on a lattice in the all *trans* conformation with the center of mass at the cubic lattice points. During this initial equilibration period the atoms are grown to full size and then allowed to equilibrate for a further 5000 ps. This equilibrium configuration provides the starting point for both the EMD and NEMD simulations. The strain rate dependant properties were calculated once the system has reached a steady state under the influence of shear flow.

3. Results

We have performed both EMD and NEMD simulations of 9-octylheptadecane at the state points given in Table 3. In addition to the rheological properties, we are also interested in a number of equilibrium properties, such as the rotational relaxation which is a useful quantity when examining the transition from Newtonian to non-Newtonian behavior. When the shear field exceeds the inverse of the longest relaxation time the system cannot respond fast enough to the deformation due to the flow field, and molecular alignment with the flow field begins to appear, which results in a reduced viscosity. Hence, the inverse of the rotational relaxation time, τ, provides a good guide to the transition from the Newtonian to non-Newtonian regime. The rotational relaxation times for 9-octylheptadecane at both state points

Table 3
State points studied

Molecule	Temperature (K)	Density (g cm^{-3})
9-Octylheptadecane	311	0.791
	372	0.751
9-Octyldocosane	311	0.800
	372	0.761
Squalane	311	0.798
	372	0.759

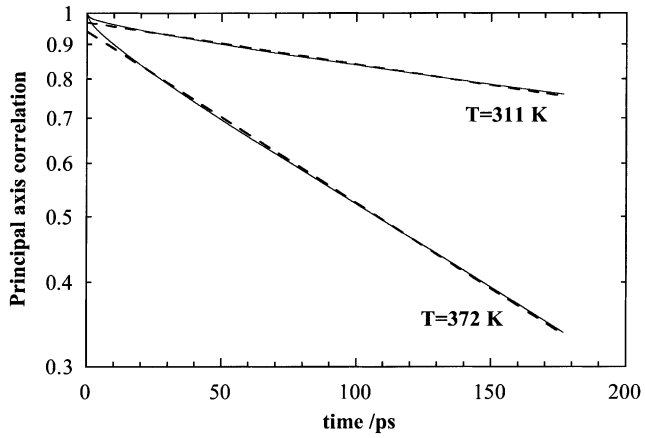

Fig. 1. Rotational relaxation of 9-octylheptadecane at 311 and 372 K. The solid lines are the simulation data and the dashed lines a fit to the data.

were determined by studying the orientational relaxation of the longest principal axis of each molecules ellipsoid of inertia. From the rate of exponential decay of the vector we can obtain the relaxation time (Fig. 1), which at 311 K gave $\tau = 702$ ps and at 372 K gave $\tau = 189$ ps, the inverse of which corresponds to strain rates of 1.4×10^9 and $5.3 \times 10^9\ s^{-1}$, respectively.

The NEMD simulations were performed over a wide range of stain rates (10^8–$10^{11}\ s^{-1}$) for both state points studied. In Fig. 2, we present the strain rate dependant viscosity as a log–log plot. In the figure, the horizontal lines correspond to the experimental zero-shear viscosity for each state point [24] and the arrows are the inverse of the rotational relaxation times estimated from the equilibrium simulations. We

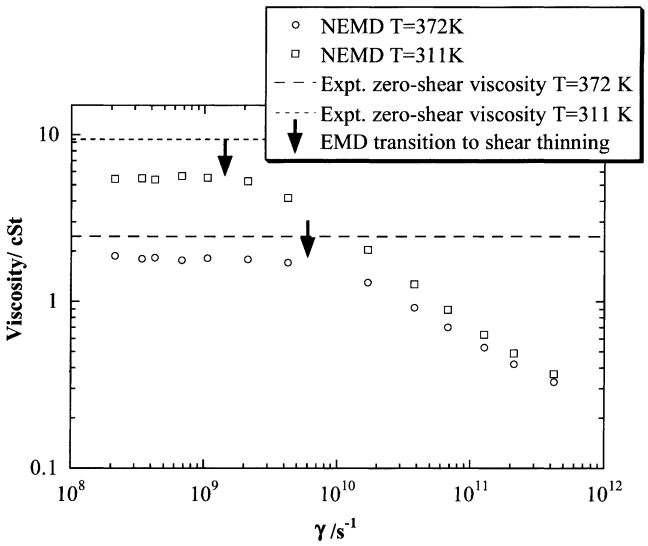

Fig. 2. Kinematic viscosity as a function of strain rate for 9-octylheptadecane at 372 and 311 K.

Table 4
Results of NEMD simulation for the VI and VN compared with experimental values

Molecule	VI_{NEMD}	$VI_{expt.}$	VN_{NEMD}	$VN_{expt.}$
9-Octylheptadecane	–	–	91(±4)	94 (±9)
9-Octyldocosane	153 (±34)[a]	143 (±45)[a]	100 (±4)	101 (±7)
Squalane	103 (±18)[b]	116 (±30)[b]	94 (±4)	97 (±7)

[a] Taken from [18].
[b] Taken from [15].

can see from Fig. 2, that the viscosity shows shear-thinning behavior at high strain rates and a Newtonian plateau at the lowest strain rates. The onset of shear thinning as the strain rate increases occurs at a higher strain rate for the higher temperature studied, which is consistent with earlier work. We also see from Fig. 2, the transition from Newtonian to non-Newtonian behavior predicted by the NEMD simulations correlates well with the inverse of the rotational relaxation time. The zero-shear viscosity can be estimated from the NEMD simulation data by averaging the values at strain rates that appear to fall within the Newtonian plateau. As anticipated, and can be seen from Fig. 2, the NEMD simulations under estimate the zero-shear viscosity, which is thought to be due to the smoothness of the united atom model compared to the real molecular architecture [18].

Given the zero-shear viscosity of 9-octylheptadecane is below 2 cSt at 100°C we were unable to determine the VI from the simulation results, though the VN is easily determined through Eqs. (1) and (2). We have calculated the VN for 9-octylheptadecane from the simulation data presented here, and for of 9-octyldocosane and 2,6,10,15,19,23-hexamethyltetracosane (squalane) from previous simulation studies at the state points given in Table 3 [18]. The predicted values of the VN are compared with experimental values in Table 4. The VNs predicted by our NEMD simulations are in excellent agreement with the experimental data. This result further supports the idea that, while NEMD simulation with this UA model under predicts the actual value of the viscosity, the model does an excellent job in predicting its temperature dependence.

4. Concluding remarks

We have presented the results of equilibrium and non-equilibrium molecular dynamics simulations for 9-octylheptadecane at 311 and 372 K. The rotational relaxation time was determined for each state point and its inverse is found to be in good agreement with the predicted transition from Newtonian to non-Newtonian behavior from the NEMD simulations. The zero-shear viscosity was estimated from the NEMD simulation results and was seen to under predict the experimental value, which is consistent with previous studies. Additionally, from the zero-shear viscosity we determined the viscosity number for 9-octylheptadecane, and for 9-octyldocosane and squalane using previous simulation results. The predicted values are in excellent agreement with the experimental result in all three cases. This provides further support for the observation that whilst the UA model under predicts the actual viscosity of these molecules, it does capture the temperature dependence. With this in mind, molecular simulation could prove invaluable to probe the rheological properties of, as yet, unsynthesized molecules, such as synthetic lubricant candidates. Although synthetic lubricants at present make up a very small percentage of the

total market this number will rise as automobile engine design pushes toward greater efficiency, reduced maintenance and emissions, which will inevitably lead to more demanding operating conditions that current lubricants are not designed to meet.

List of symbols

a_i	parameters in torsional potential
A, B	coefficients in Walther equation, Eq. (1)
k	spring constant in intramolecular interactions
k_B	Boltzmann's constant
T	temperature
VI	viscosity index
VN	viscosity number

Greek letters

ε	energy parameter in Lennard–Jones interaction
γ	strain rate
θ	angle between adjacent C–C bonds in an alkane chain
σ	distance parameter in Lennard–Jones interaction
τ	orientational relaxation time

Acknowledgements

The authors would like to thank J.D. Moore for assistance in the early stages of this work. This work was supported in part by the Division of Materials Sciences of the US Department of Energy. Oak Ridge National Laboratory is operated for the Department of Energy by Lockheed Martin Energy Research Corporation under Contract No. DE-AC05-96OR22464. Additional funding was provided by Mobil Technology Company.

References

[1] H.H. Zuidema, The performance of Lubricating Oils, Reinhold, New York, 1959.
[2] E.W. Dean, G.H.B. Davis, Chem. Met. Eng. 36 (1929) 618–619.
[3] E.W. Hardiman, A.H. Nissan, J. Inst. Pet. 31 (1945) 255–271.
[4] M. Sanchez-Rubio, A. Heredia-Veloz, J.E. Puig, S. Gonzalez-Lozano, Lubricat. Eng. 48 (1992) 821–826.
[5] P.T. Cummings, D.J. Evans, Ind. Eng. Chem. Res. 31 (1992) 1237–1252.
[6] R. Edberg, G.P. Morris, D.J. Evans, J. Chem. Phys. 86 (1987) 4555–4570.
[7] G.P. Morris, J. Chem. Phys. 94 (1991) 7420–7433.
[8] A. Berker, S. Chynoweth, U.C. Klomp, Y. Michopoulos, J. Chem. Soc., Faraday Trans. 88 (1992) 1719–1725.
[9] C.J. Mundy, J.I. Siepmann, M.L. Klein, J. Chem. Phys. 102 (1994) 3376–3380.
[10] S.T. Cui, P.T. Cummings, H.D. Cochran, J. Chem. Phys. 104 (1996) 255–262.
[11] S.T. Cui, S.A. Gupta, P.T. Cummings, J. Chem. Phys. 105 (1996) 1214–1220.
[12] C.J. Mundy, S. Balasubramanian, K. Bagchi, J.I. Siepmann, M.L. Klein, Faraday Trans. 104 (1996) 17–36.
[13] K.P. Travis, D.J. Evans, Mol. Sim. 17 (1996) 157–164.
[14] R. Khare, J. de Pablo, A. Yethiraj, J. Chem. Phys. 107 (1997) 6956–6964.
[15] J.D. Moore, S.T. Cui, P.T. Cummings, H.D. Cochran, AIChE J. 43 (1997) 3260–3263.

[16] M. Mondello, G.S. Grest, E.B. Webb, P. Peczak, J. Chem. Phys. 109 (1998) 798–805.
[17] L.I. Kioupis, E.J. Maginn, J. Phys. Chem. B 103 (1999) 10781–10790.
[18] J.D. Moore, S.T. Cui, H.D. Cochran, P.T. Cummings, J. Chem. Phys. 113 (2000) 8833–8840.
[19] J.I. Siepmann, S. Karaborni, B. Smit, Nature 365 (1993) 330–332.
[20] B. Smit, S. Karaborni, J.I. Siepmann, J. Chem. Phys. 102 (1995) 2126–2140.
[21] M. Mondello, G.S. Grest, J. Chem. Phys. 103 (1995) 7156–7165.
[22] M.E. Tuckerman, B.J. Berne, G.J. Martyna, J. Chem. Phys. 97 (1992) 1990–2001.
[23] S.T. Cui, P.T. Cummingsm, H.D. Cochran, J. Chem. Phys. 104 (1996) 255–262.
[24] API 42: Properties of Hydrocarbons of High Molecular Weight, American Petroleum Institute, New York, 1966.